

Contents lists available at ScienceDirect

Journal of Energy Chemistry

journal homepage: www.elsevier.com/locate/jechem



http://www.journals.elsevier.com/

Water effect on band alignment of GaP: A theoretical insight into pyridinium catalyzed CO_2 reduction^{$^{\circ}$}

Xue-Ting Fan^a, Mei Jia^a, Ming-Hsien Lee^b, Jun Cheng^{a,c,*}

- ^a State Key Laboratory of Physical Chemistry of Solid Surfaces, iChEM, College of Chemistry and Chemical Engineering, Xiamen University, Xiamen 361005, Fujian, China
- ^b Department of Physics, Tamkang University, New Taipei 25137, Taiwan, China
- ^c Department of Chemistry, University of Aberdeen, Aberdeen AB24 3UE, UK

ARTICLE INFO

Article history: Received 9 January 2017 Revised 26 February 2017 Accepted 3 March 2017 Available online 9 March 2017

Keywords:
Band alignment
GaP
Pyridinium
CO₂ reduction
DFT

ABSTRACT

GaP has been shown to have good photo-catalytic activity in pyridinium catalyzed CO_2 reduction. The photo-excited electrons in the conduction band of GaP should have a sufficient reduction potential to drive the reduction of pyridinium and CO_2 . In this work, we have studied water adsorption on the GaP surface using density functional theory calculations, and its effect on the band alignment. Our calculations have shown that there are surface states present near the band edges due to unsaturated dangling bonds, and water adsorption can remove these states partially or almost completely depending on the adsorption states of water. More importantly, we have found that water adsorption has considerable effects on the band alignment, shifting up the band positions by up to 0.5 eV compared to the bare surface. The computed level of the conduction band with the adsorption of water is rather close to the reduction level of pyridinium ions, thus suggesting that photo-excited electrons are thermodynamically possible to reduce pyridinium to pyridinyl radicals that further help CO_2 reduction.

© 2017 Science Press and Dalian Institute of Chemical Physics, Chinese Academy of Sciences. Published by Elsevier B.V. and Science Press. All rights reserved.

1. Introduction

Environmental pollution and energy crisis are two major global problems we are facing today. Carbon based fossil fuels are the main source of energy for human kind. They are limited and the sustainable use of carbon resources is a critical issue that we need to address. On the other hand, their consumption results in increasing level of CO_2 in atmosphere, which is believed to be responsible for global warming [1]. Conversion of CO_2 to products with added values is an appealing means to address environment and energy challenges simultaneously. The conversion is usually thermodynamically unfavorable, and CO_2 reduction needs to be driven by supplying extra energy in the form of electricity [2–4] or light [5–7].

Most of studied systems reduce CO₂ to CO and/or hydrocarbons, while fewer studies have been targeted at the high value product

E-mail addresses: chengjun@xmu.edu.cn, jcheng@abdn.ac.uk (J. Cheng).

CH₃OH that is more desirable due to an obvious economic reason. It has been reported that hydrogenated Pd [8], Pt [9], p-GaP [10], Pt/C-TiO₂ [11] and so on can reduce CO₂ to methanol at low overpotentials. Bocarsly and co-workers have found that the electrochemical reduction of CO₂ to methanol occurs at a low overpotential in the presence of pyridinium (PyH⁺) [8]. Interestingly, the photoelectrochemical cell with p-GaP as a photoelectrode can yield CH₃OH with 100% faradaic efficiency at an underpotential of 300 mV [10]. It is considered the first system capable of reducing CO₂ to methanol using only the energy of light. This is particularly attractive, as photoelectrochemical reduction of CO₂ to liquid fuels by solar energy could potentially complete the environmentally friendly carbon-neutral cycle for the world energy consumption.

Understanding Py-catalyzed CO₂ reduction in p-GaP photocatalytic system is of great importance. Elucidating the catalytic role of Py and p-GaP may help develop more effective catalysts. The underlying mechanism has been investigated experimentally and theoretically. Bocarsly and co-workers first reported the detailed mechanism [9], and suggested that Pyridinyl radical plays an important role in CO₂ reduction to methanol. However, theoretical calculations [12,13] indicated that pyridinium reduction having a rather negative redox potential is thermodynamically unfavorable and thus other possible mechanisms were proposed [14–22]. It is worth mentioning that Musgrave and co-workers argued

 $^{^{\,\}dot{\,}}$ This work was supported by the National Natural Science Foundation of China (Grant No. 21373166 and 21621091) and the Thousand Youth Talents Program of China

^{*} Corresponding author at: State Key Laboratory of Physical Chemistry of Solid Surfaces, iChEM, College of Chemistry and Chemical Engineering, Xiamen University, Xiamen 361005, Fujian, China.

that photo-excited electrons might have sufficient energy to reduce PyH⁺ when using p-GaP photoelectrodes [15].

What makes a semi-conductor a potential candidate for pyridinium reduction is its conduction band minimum (CBM) being higher than the reduction level of pyridinium. Carter and coworkers [23,24] calculated the electronic energy levels and found that the computed CBM of GaP(110) surface lies too low to transfer photoexcited electrons to pyridinium. However, their calculation model is a bare GaP surface without accounting for water hydration effects, and the obtained CBM is about 0.5 eV below the experimental value [25]. It has been shown that hydration can have significant impact on the level alignment across semiconductor water interface [26,27]; in particular, the band positions of rutile $TiO_2(110)$ can be shifted up by \sim 1.5 eV when interacting with water. In this work, we attempt to investigate the contribution of surface water to band alignment of GaP(110).

The paper is organized as follows. Computational details are summarized in Section 2. Results on state of adsorbed water, band alignment of GaP(110) surface are shown in Section 3, followed by discussion on comparison between band positions and the redox level of pyridinium. We finish this paper with some conclusions in the end.

2. Computational details

The GaP(110) surface was modeled by periodic slabs with lateral dimensions of a 2×3 surface cell. The slabs were separated by a space of 15 Å leading to an orthorhombic super-cell of $10.9 \times 11.5 \times 22.7$ ų. Full 3D periodic boundary conditions (PBC) were applied. Adsorbates were modeled symmetrically above and below GaP(110) slabs so that no dipole corrections due to periodic images in the *z*-direction were needed. All the atoms in the cell were relaxed during geometry optimization.

All density functional theory (DFT) calculations were carried out using the freely available program package CP2K/Quickstep [28]. The DFT implementation in Quickstep is based on a hybrid Gaussian plane wave (GPW) scheme. Orbitals are described by an atomcentered Gaussian-type basis set, while an auxiliary plane wave basis is used to re-expand the electron density [29]. The wave function optimization is performed using an efficient orbital transformation minimizer, which avoids the traditional matrix diagonalization method and gives optimal convergence control [30]. Analytic Goedecker-Teter-Hutter (GTH) pseudopotentials [31,32] were employed to represent the core electrons. The basis sets for the valence electrons $(2s^22p^4)$ for O, $1s^1$ for H, $3d^{10}4s^2$ $4p^1$ for Ga and $3s^2$ $3p^3$ for P) consist of short-ranged (less diffuse) double- ζ basis functions with one set of polarization functions (DZVP) [33]. The gradient-corrected Perdew-Burke-Ernzerhof (GGA-PBE) functional [34] was used for all calculations with the Grimme's dispersion correction [35]. The plane wave basis for the electron density expansion is cut off at 400 Ry. All the simulations only used the Γ point of the supercell for expansion of the orbitals considering the large size of the cell. The convergence criterion for wave function optimization was set by a maximum electronic gradient of 3×10^{-7} a.u. and an energy difference tolerance between selfconsistent field (SCF) cycles of 10^{-13} a.u.

3. Results and discussion

In this study, we aim to determine the positions of conduction band minimum (CBM) and valence band maximum (VBM) of the GaP(110) surface, which is of importance to the photocatalytic activity of GaP in $\rm CO_2$ reduction in the presence of pyridinium. It has been shown that adsorption of one monolayer (ML) of water on rutile $\rm TiO_2(110)$ can lift up the band positions by ~ 1.5 eV [26].

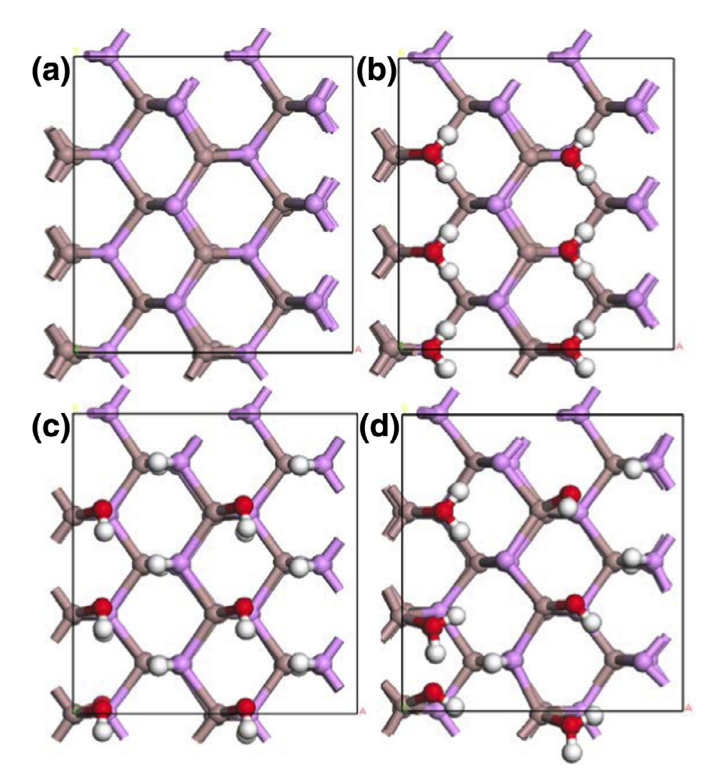


Fig. 1. (a) Top views of the bare GaP(110) surface and different adsorption states of monolayer (ML) of H_2O on GaP(110) surface: (b) associative adsorption; (c) fully dissociative adsorption; (d) a mixed state with half water associative adsorbed and half water dissociative adsorbed. Adsorption is symmetric above and below the slab under full geometry relaxation. Ga, P, O, and H atoms are distinguished in brown, purple, red, and white, respectively. (For interpretation of the references to colour in this figure legend, the reader is referred to the web version of this article.)

Therefore, we have investigated water adsorption on the GaP surface, and its effect on band alignment.

3.1. States of adsorbed water on the GaP(110) surface

As shown in Fig. 1, we have calculated three representative adsorption states of 1 ML of water on the GaP surface, namely, the molecular adsorption, the fully dissociative adsorption and the mixed adsorption state with half water molecularly adsorbed and half water dissociatively adsorbed, respectively. Different kinds of adsorption states may lead to different band edge positions and band gaps of the GaP(110)-1 ML surface. Thus, we set off to find out the most stable adsorption states of monolayer (ML) of H₂O on GaP(110) surface first. We have also calculated the adsorption energies with different layers of the GaP slab to investigate the convergence of water adsorption against the slab thickness. The water adsorption energies in Fig. 2 were calculated using the following equation,

$$E_{ad} = \frac{E_{slab+water} - E_{slab} - nE_{water}}{n}$$

where $E_{\rm ad}$, $E_{\rm slab+water}$, $E_{\rm slab}$ and $E_{\rm water}$ denote water adsorption energies, the total energies of slab+water systems, the total energy of the bare slab, the total energy of a water molecule in the gas phase, and n is the number of water molecules adsorbed on the surface

From Fig. 2, we can see the adsorption energies of all three water states remain almost constant when increasing the number of layers of the GaP slab. The difference between adsorption energies of dissociated water and molecular water on the GaP surface is small. A mixed state with half associative and half dissociative

Table 1. Variation of the band alignment of the clean GaP(110) surface in vacuum and the surfaces with the adsorption of 1 ML of H_2O as a function of the number of GaP layers^a.

No. of GaP layers	No water			1 ML H ₂ O _{ass.}			1 ML H ₂ O _{mix.}			1 ML H ₂ O _{diss.}		
	VBM	CBM	Band gap	VBM	CBM	Band gap	VBM	CBM	Band gap	VBM	CBM	Band gap
5	0.74	-0.75	1.49	0.49	-1.13	1.62	0.48	-1.26	1.74	0.75	-1.22	1.97
7	0.74	-0.69	1.43	0.47	-1.14	1.61	0.41	-1.22	1.63	0.69	-1.11	1.80
9	0.74	-0.73	1.47	0.50	-1.14	1.64	0.37	-1.26	1.63	0.67	-1.06	1.73
11				0.50	-1.14	1.64				0.64	-1.07	1.71

a The band gaps are in eV, and the band positions are in V versus SHE. The calculated band gap of bulk GaP is 1.64 eV. All the energies are calculated using the PBE functional. The experimental CBM and VBM are −1.26 V and 0.98 V versus SHE, respectively, with a band gap of 2.2 eV [25].

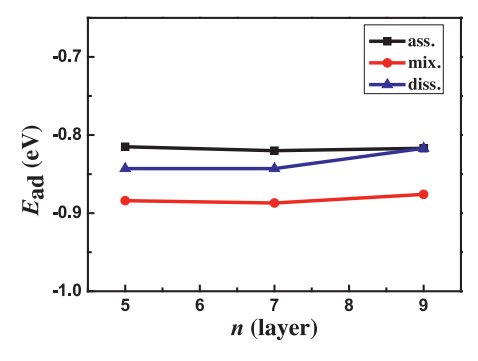


Fig. 2. The adsorption energy (eV per molecule) of water on GaP(110) in vacuum against the number of GaP layers. Three adsorption states of 1 monolayer (ML) of H_2O on the GaP(110) surface are considered, namely, associative (ass.), dissociative (diss.), and mixed (mix) with half associative and half dissociative, as shown in Fig. 1.

adsorption appears to be slightly more stable than the fully dissociative and molecular adsorption states based on our total energy calculations.

3.2. The effects of water adsorption on electronic structures of GaP surfaces

Variation of the band edge positions of the bare GaP(110) surface and the surface with the adsorption of 1 ML H₂O with the different slab thickness has been investigated, and the results are presented in Fig. 3 and Table 1. The absolute positions are obtained by referencing the highest occupied molecular orbitals (HOMO) and the lowest unoccupied molecular orbitals (LUMO) to the vacuum level, and they can be converted into the standard hydrogen electrode (SHE) by subtracting the absolute SHE potential of 4.44 V [36-38].

We first analyze the band alignment of GaP(110) clean surface using the PBE functional. As shown in Fig. 3(a) and Table 1, the VBM and CBM positions remained rather constant against the slab thicknesses, and a 5-layer slab appears sufficient to converge the band positions, i.e. 0.74 V and -0.75 V versus SHE for VBM and CBM, respectively, with a gap of 1.49 eV. Compared to the bulk band gap of 1.64 eV computed with the same PBE functional, it decreases by 0.15 eV, presumably due to the formation of surface states near the band edges. An apparent fast convergence of band positions has also been found on the GaP surface with 1 ML associative adsorption of molecular water. The VBM and CBM are 0.5 V and -1.1 V versus SHE, giving rise to a gap of 1.6 eV that is quite close to the bulk band gap. Note that there are 0.2 V and 0.4 V upshifts in VBM and CBM, respectively, in the present of water adsorption. Also, the water adsorption states have some effects on the band edges and their convergences against the slab thickness. For example, for the mixed adsorption state, a 7-layer slab gives the converged results. While in the case of dissociative adsorption, the convergence is slower. A 9-layer slab gives a band gap of 1.73 eV, still 0.1 eV larger than bulk value. In fact, with dissociatively adsorbed water the band gaps of the slabs from 5 layers to 11 layers are all larger than the band gap in bulk, slowly converging to the bulk value. This cannot be explained by the presence of surface states as they usually lead to smaller band gaps (see the results of the bare surface).

To understand these results, we have calculated the density of states (DOS) of the surfaces. In Fig. 4, we show the projected DOS plots of the bulk, the 5-layer bare surface and those with three water adsorption states. Comparing the DOS plots of the bulk GaP and the bare surface (see Fig. 4(a), and (b)), it is clear that there are considerable amount of electronic states mainly consisting of the orbitals of the surface Ga and P atoms near the CBM. They can be attributed to the dangling covalent bonds of the unsaturated Ga and P atoms on the surface. The adsorption of water significantly annihilates the surface states, as evidenced in Fig. 4(c), (d) and (e). This must result from the fact bonding with water can reduce the degree of unsaturation of the surface atoms. Furthermore, the extent of reduction is related to the water adsorption states: dissociative adsorption reduces the most, while associative adsorption reduces the least, with the mixed state in between. This is expected because molecular water only binds on the Ga atoms, leaving the surface P atoms remaining unsaturated, and H atoms can bind with the P atoms when water dissociates. Therefore, the water adsorption widens up the band gaps of the 5-layer GaP slabs, the extent of which follows the order: dissociative > mixed > associative.

However, the mixed adsorption state gives a band gap of 1.74 eV, slightly larger than the bulk value (1.64 eV), and the fully dissociative adsorption even increases the band gap to 1.97 eV. Thus, the widening of the surface band gaps for the 5-layer slab cannot be simply attributed to the disappearance of the dangling bond states. We then compare the DOS of 5-layer and 11-layer GaP surfaces with dissociative adsorption of water together with the bulk GaP, as shown in Fig. 5. It is evident that there are some electronic states missing at the edge of conduction band on the 5-layer slab, and they show up on the 11-layer slab. This can be regarded as a finite size effect owing to too small slab thickness that leads to insufficient representation of the band states normal to the surface. To further show this, we plot the DOS of 5-, 7-, 9- and 11-layer slabs in Fig. 6. We can see that the number of states near the CBM increases gradually from 5-layer to 11-layer, resulting in a noticeable downshift of CBM of 0.15 eV. A similar effect is also seen for the VBM, while the magnitude is somewhat smaller. On the other hand, the projection of the DOS on the surface atoms hardly contributes to the states at the band edges according to Fig. 6, further demonstrating that it is indeed a finite size effect. This however is in contrast to the case of associative adsorption in which the presence of surface states near band edges clearly affects the band positions and band gap (see Fig. 4(c)).

The computed CBM and VBM positions of the bare GaP surface and the surfaces with the adsorption of 1 ML H_2O are shown in Fig. 7. These are converged values against the number of layers of the GaP slab, which are 5, 5, 7, 9 layers corresponding to the slabs without water adsorption, with associative, mixed, dissociative adsorption of water, respectively. Note that faster convergence

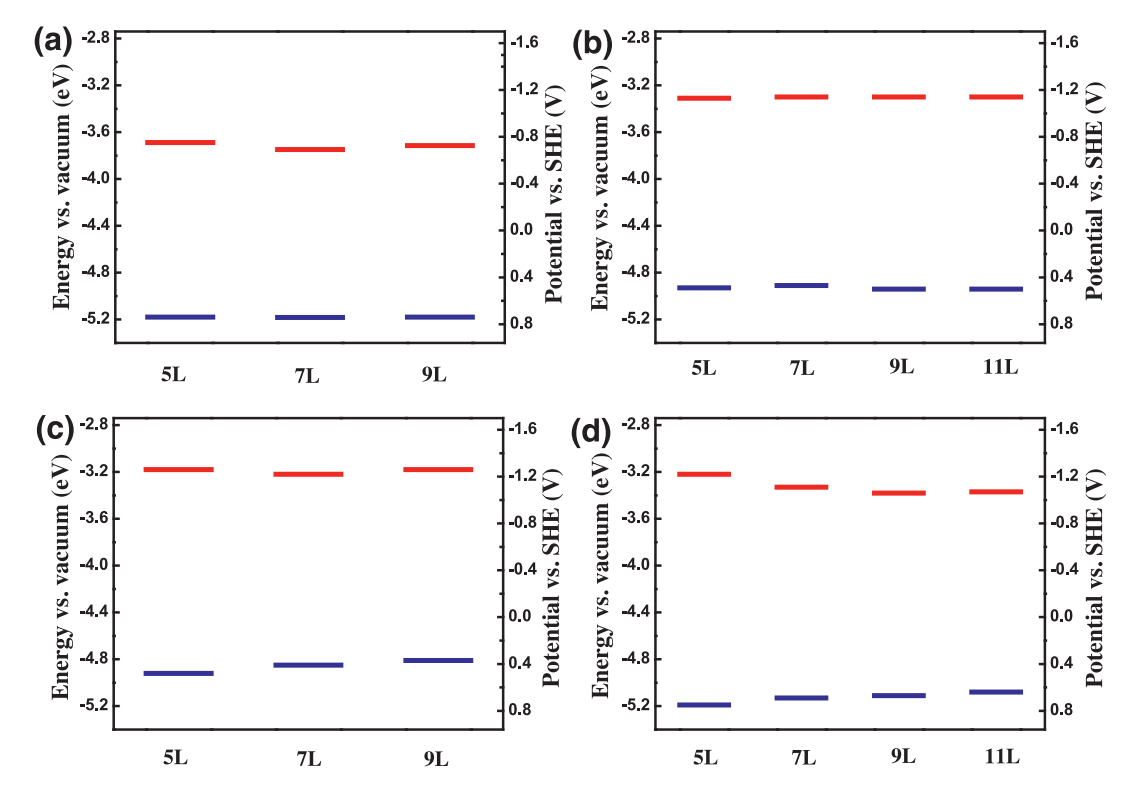


Fig. 3. Level alignment of electronic band edges of the GaP(110) surfaces against the number of the layers of the slab: (a) the clean surface, and the surfaces with the adsorption of 1 ML H_2O ((b) associative, (c) mixed, and (d) dissociative). Values on the vacuum scale are converted to the SHE scale using the absolute potential of the standard hydrogen electrode of 4.44 V [36-38].

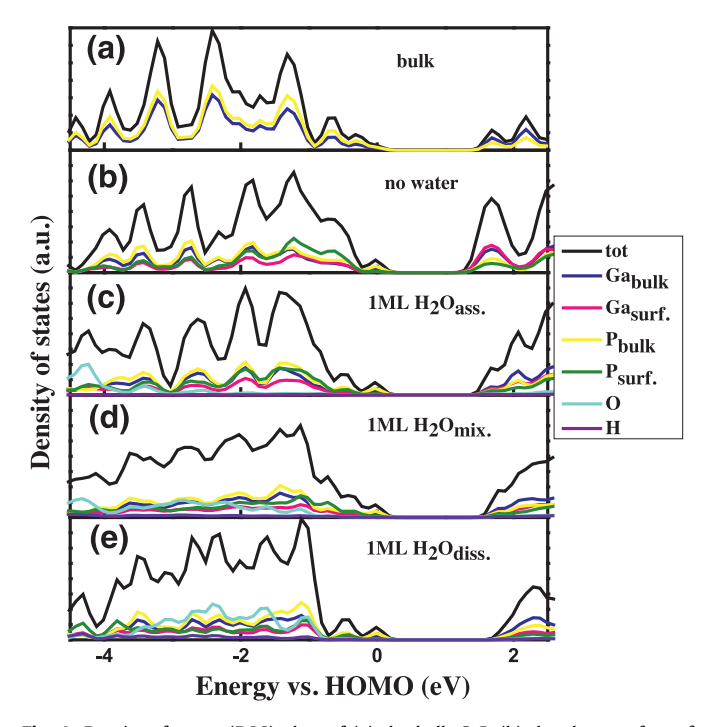


Fig. 4. Density of states (DOS) plots of (a) the bulk GaP, (b) the clean surface of 5-layer GaP(110) in vacuum, and the 1 ML $\rm H_2O$ adsorbed 5-layer GaP(110) surfaces ((c) associative, (d) mixed, and (e) dissociative). The DOS have been projected in separate to the surface/bulk Ga and P atoms (see the legend for the color code). They are calculated using the PBE functional, and energy zero is set to the highest occupied molecular orbital (HOMO).

against slab thickness for the former three cases is owing to the pinning of surface states, while in the fourth case (dissociative) where the surface states are largely eliminated, thicker slabs are

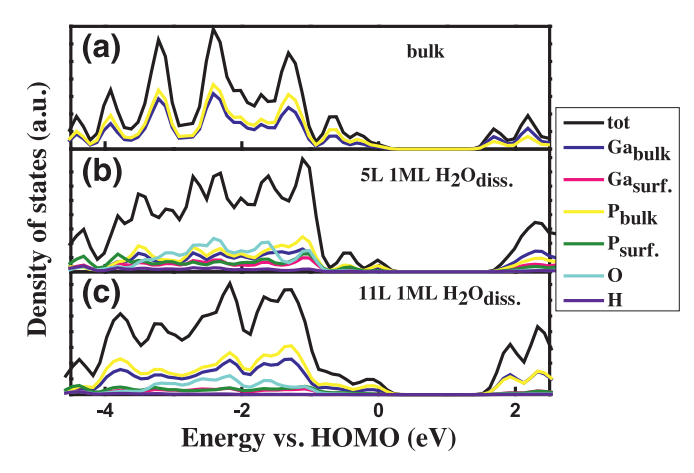


Fig. 5. Density of states (DOS) plots of (a) the bulk GaP, and the GaP(110) surfaces with dissociative adsorption of 1 ML ((b) 5-layer slab and (c) 11-layer slab). The DOS have been projected in separate to the surface/bulk Ga and P atoms (see the legend for the color code). They are calculated using the PBE functional, and energy zero is set to the highest occupied molecular orbital (HOMO).

needed to converge the band positions and gap. More importantly, we can conclude from Fig. 7 that water adsorption and the adsorption states clearly have considerable effect on the band positions, although the effect, on the order of 0.2–0.5 eV, is modest compared to TiO_2 in which shift of \sim 1.5 eV in band positions has been shown upon water adsorption [26].

Finally, we comment on the accuracy of the PBE functional on the band positions. As expected from the well-known delocalization error in this functional, the bulk band gap (1.64 eV) is underestimated, by $\sim\!\!0.6\,\text{eV}$, compared to the experimental value of 2.2 eV. Having little information on surface condition in experiment, it is not possible to make direct comparison between band

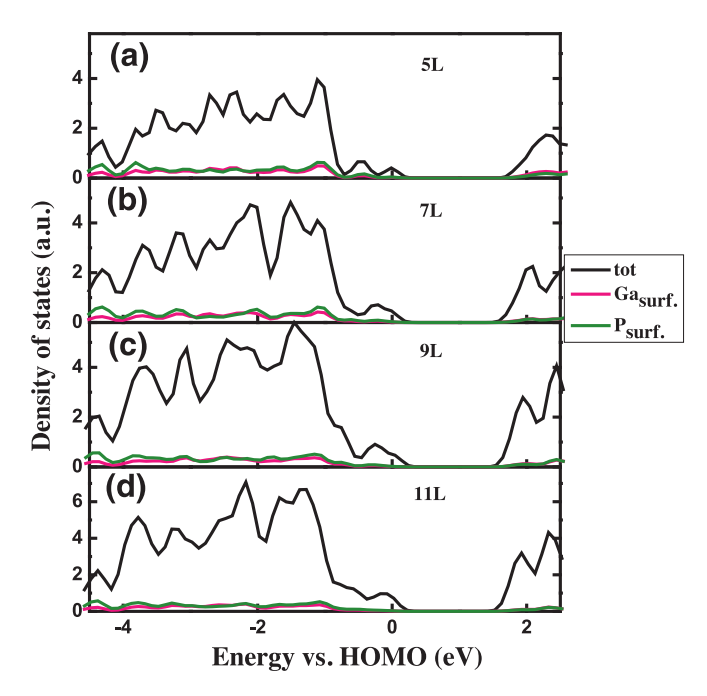


Fig. 6. Density of states of 1 ML H_2O dissociative adsorbed on the (110) surface of GaP for different atomic layer thick slabs: 5 layer (top); 7 layer (second); 9 layer (third); and 11 layer (bottom) using the GGA-PBE functional. Zero energy is aligned to the HOMO. The total density of states is indicated by the black curve, while density of states projected on surface Ga and P atoms are indicated by red and green curve respectively. (For interpretation of the references to colour in this figure legend, the reader is referred to the web version of this article.)

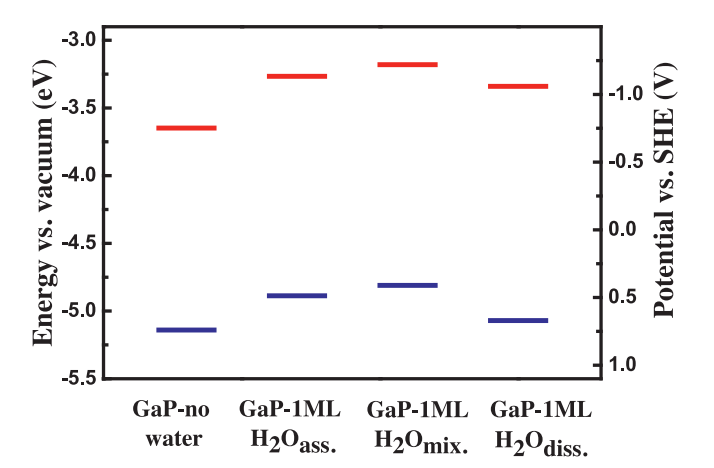


Fig. 7. Computed conduction band and valence band edges of the bare GaP surface (5-layer) compared, and the surfaces with the adsorption of 1 ML $\rm H_2O$ (associative adsorption (5-layer slab), mixed adsorption (7-layer slab), and dissociative adsorption (9-layer slab)). Values on the vacuum scale are converted to the SHE scale using the absolute potential of the standard hydrogen electrode of 4.44 V [36–38].

positions. It is however worth noting from Table 1 that the computed CBM with water adsorption is quite close to experimental value (\sim -1.2 V versus SHE), leaving the majority error present in the VBM. Similar has been observed in TiO₂ [26] and GaN [27]. Another proof to this claim is that the CBM of the bare GaP surface computed by Carter and co-workers using the G₀W₀ theory [24] is -0.71 V versus SHE, essentially the same as the PBE value.

3.3. Photo-catalytic activity of GaP

The photocatalytic activity of GaP in CO_2 reduction in the presence of pyridinium (PyH $^+$) is related to its CBM relative to the pyridinium reduction level. For the photo-excited electrons to pro-

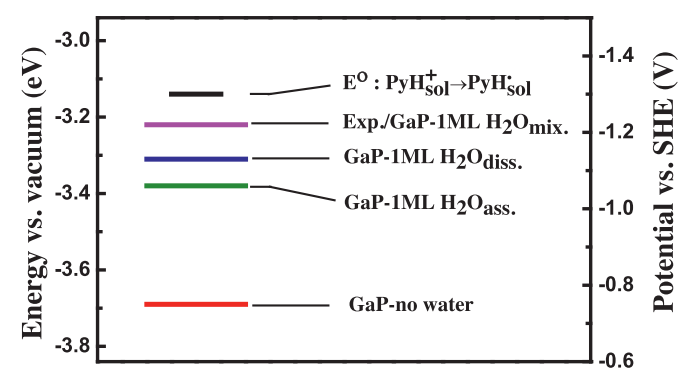


Fig. 8. Comparison of the computed conduction band minimums (CBM) under various surface conditions with the reduction potential of PyH⁺. The experimental GaP CBM is taken from [25], and the computed PyH⁺/PyH⁺ potential from [12,13].

vide sufficient thermodynamic driving force to reduce pyridinium ions, the GaP CBM needs to be located at a higher position than the reduction level of PyH+/PyH*. Carter and coworkers have calculated the CBM in comparison to the PyH+/PyH* potential and concluded that the CBM lies too low to reduce the PyH+ ions [24]. However, the bare GaP surface was used without taking into account the effect of water adsorption. Also, the computed CBM is about 0.5 eV lower than the experimental estimate (-0.71 V versus -1.26 V with respect to SHE) [24,25].

As discussed above, surface hydration has a considerable effect on the band alignment, and adsorption of 1 ML water can push up the GaP CBM by up to 0.5 eV, bringing the value close to experiment. The computed PyH+/PyH+ potential is -1.3 V versus SHE, and together with the computed GaP CBM positions with various surface conditions are compared in Fig. 8. It is clear that the surface with mixed adsorption state, most consistent with experiment, gives a CBM just less than 0.1 eV below the computed PyH+/PyH+ potential level. The close proximity cannot rule out the possibility that the conduction band electrons of GaP are capable of reducing PyH+ to PyH+ which further help facilitate CO₂ reduction.

It is evident from our calculations that hydration effect is important to the band alignment. However, we need to point out that in this work we only use a model with adsorption of 1 ML water. To realistically represent hydration effect, we will need to set up a full GaP(110)-water interface model, and use sampling techniques such as molecular dynamics to properly account for the dynamic behavior of solid-aqueous interfaces [26,39–42]. This is currently under study, and will be reported in future.

4. Conclusions

GaP is a good photocatalyst for CO_2 reduction with a high selectivity toward methanol. However, the role of GaP photocathodes in pyridinium-catalyzed CO_2 reduction is not clear. In this work, we have studied water adsorption on the $\mathrm{GaP}(110)$ surface using DFT calculations, and its effect on the band alignment that is relevant to the mechanism of pyridinium-catalyzed CO_2 reduction. The following conclusions have been reached.

- (i) Computation of water adsorption energies quickly converges against the slab thickness with a 5-layer slab being already sufficient. It is found that a mixed state with half water associative and half dissociative adsorption is slightly more stable than the fully associative/dissociative adsorption.
- (ii) Water adsorption has rather complex impact on the electronic structures of the GaP surfaces. Surface states owing to unsaturated dangling bonds are present near the band edges on the bare surface and the surfaces with associative

- and mixed states of water adsorption, leading to fast convergence of band positions against slab thickness. The bare surface even has a band gap smaller than the bulk value. Full dissociation of water gives rise to OH binding to surface Ga, and H binding to surface P, largely eliminating the unsaturated dangling bonds and surface states. A thicker slab is needed to converge the band positions due to missing of band states perpendicular to the surface.
- (iii) Water adsorption can lift up the GaP band positions by up to 0.5 eV compared to the bare surface. The conduction band minimum computed using the PBE functional is in agreement to experimental estimate, and the error in underestimating the band gap with this functional mainly comes from the too high valence band position. Only after taking into account the effect of water, the computed conduction band minimum lies close to the reduction potential of pyridinium ions, and thus it is thermodynamically possible that the photo-exited electrons in GaP is able to reduce pyridinium to pyridinyl radical that helps facilitate CO2 reduction.

References

- [1] S.C. Roy, O.K. Varghese, M. Paulose, C.A. Grimes, ACS Nano 4 (2010) 1259-1278.
- [2] J.K.W. Frese, Electrochemical Reduction of CO₂ at Solid Electrodes, Elsevier, Amsterdam, 1993.
- [3] B.J. Fisher, R. Eisenberg, J. Am. Chem. Soc. 102 (1980) 7361-7363.
- [4] E.E. Benson, C.P. Kubiak, A.J. Sathrum, J.M. Smieja, Chem. Soc. Rev. 38 (2009) 89-99.
- [5] J.M. Lehn, R. Ziessel, Proc. Natl. Acad. Sci. 79 (1982) 701-704.
- [6] J. Hawecker, J.M. Lehn, R. Ziessel, Helv. Chim. Acta 69 (1986) 1990–2012.
- [7] J. Chauvin, F. Lafolet, S. Chardon-Noblat, A. Deronzier, M. Jakonen, M. Haukka, Chem. Eur. J. 17 (2011) 4313–4322.
- [8] G. Seshadri, C. Lin, A.B. Bocarsly, J. Electroanal. Chem. 372 (1994) 145-150.
- [9] E. Barton Cole, P.S. Lakkaraju, D.M. Rampulla, A.J. Morris, E. Abelev, A.B. Bocarsly, J. Am. Chem. Soc. 132 (2010) 11539-11551.
- [10] E.E. Barton, D.M. Rampulla, A.B. Bocarsly, J. Am. Chem. Soc. 130 (2008) 6342-6344.

- [11] N.R. de Tacconi, W. Chanmanee, B.H. Dennis, F.M. MacDonnell, D.J. Boston, K. Rajeshwar, Electrochem, Solid-State Lett. 15 (2011) B5-B8.
- [12] I.A. Tossell, Comput. Theory Chem. 977 (2011) 123-127.
- [13] J.A. Keith, E.A. Carter, J. Am. Chem. Soc. 134 (2012) 7580-7583.
- [14] Y. Yan, E.L. Zeitler, J. Gu, Y. Hu, A.B. Bocarsly, J. Am. Chem. Soc. 135 (2013) 14020-14023
- [15] C.H. Lim, A.M. Holder, C.B. Musgrave, J. Am. Chem. Soc. 135 (2013) 142-154.
- [16] E. Lebègue, J. Agullo, M. Morin, D. Bélanger, ChemElectroChem 1 (2014) 1013-1017.
- [17] J.A. Keith, E.A. Carter, Chem. Sci. 4 (2013) 1490-1496.
- [18] M.Z. Ertem, S.J. Konezny, C.M. Araujo, V.S. Batista, J. Phys. Chem. Lett. 4 (2013) 745-748.
- [19] C. Costentin, J.C. Canales, B. Haddou, J.M. Saveant, J. Am. Chem. Soc. 135 (2013) 17671-17674
- [20] D.J. Boston, C. Xu, D.W. Armstrong, F.M. MacDonnell, J. Am. Chem. Soc. 135 (2013) 16252-16255.
- [21] C.H. Lim, A.M. Holder, J.T. Hynes, C.B. Musgrave, J. Am. Chem. Soc. 136 (2014) 16081-16095
- [22] Y. Yan, J. Gu, A.B. Bocarsly, Aerosol Air Qual. Res. 14 (2014) 515-521.
- [23] J.A. Keith, A.B. Muñoz-García, M. Lessio, E.A. Carter, Top. Catal. 58 (2015) 46-56
- [24] M. Lessio, E.A. Carter, J. Am. Chem. Soc. 137 (2015) 13248–13251.[25] J.L. White, M.F. Baruch, J.E. Pander III, Y. Hu, I.C. Fortmeyer, J.E. Park, T. Zhang, K. Liao, J. Gu, Y. Yan, T.W. Shaw, E. Abelev, A.B. Bocarsly, Chem. Rev. 115 (2015) 12888-12935.
- [26] J. Cheng, M. Sprik, Phys. Rev. B 82 (2010) 081406.
- [27] A.C. Meng, J. Cheng, M. Sprik, J. Phys. Chem. B 120 (2016) 1928–1939.
- [28] J. VandeVondele, M. Krack, F. Mohamed, M. Parrinello, T. Chassaing, J. Hutter, Comput. Phys. Commun. 167 (2005) 103-128. www.cp2k.org.
- [29] B.G. Lippert, J.H. Parrinello, Michele, Mol. Phys. 92 (1997) 477-488.
- [30] J. VandeVondele, J. Hutter, J. Chem. Phys. 118 (2003) 4365–4369.
- [31] S. Goedecker, M. Teter, J. Hutter, Phys. Rev. B 54 (1996) 1703.
- C. Hartwigsen, S. Goedecker, J. Hutter, Phys. Rev. B 58 (1998) 3641-3662.
- J. VandeVondele, J. Hutter, J. Chem. Phys. 127 (2007) 114105.
- [34] J.P. Perdew, K. Burke, M. Ernzerhof, Phys. Rev. Lett. 77 (1996) 3865-3868.
- [35] S. Grimme, J. Antony, S. Ehrlich, H. Krieg, J. Chem. Phys. 132 (2010) 154104.
- S. Trasatti, Pure Appl. Chem. 58 (1986) 955-966.
- [37] W.R. Fawcett, Langmuir 24 (2008) 9868-9875.
- [38] M.H. Tissandier, K.A. Cowen, W.Y. Feng, E. Gundlach, M.H. Cohen, A.D. Earhart, J.V. Coe, J. Phys. Chem. A 102 (1998) 7787-7794.
- [39] J. Cheng, M. Sprik, J. Chem. Theory Comput. 6 (2010) 880-889.
- [40] J. Cheng, X. Liu, J. VandeVondele, M. Sulpizi, M. Sprik, Acc. Chem. Res. 47 (2014) 3522-3529.
- [41] J. Cheng, M. Sulpizi, M. Sprik, J. Chem. Phys. 131 (2009) 154504.
- [42] J. Cheng, M. Sprik, Phys. Chem. Chem. Phys. 14 (2012) 11245–11267.